

Short Communication

Porous Honeycomb-like Carbon Prepared by a Facile Sugar-Blowing Method for High-Performance Lithium-Sulfur Batteries

Wenxiao Su², Wangjun Feng^{1,2,*}, Yue Cao², Linjing Chen², Miaomiao Li², Changkun Song²

¹ State Key Laboratory of Advanced Processing and Recycling Nonferrous Metals, Lanzhou University of Technology, Lanzhou 730050, China;

² School of Science, Lanzhou University of Technology, Lanzhou 730050, China)

*E-mail: wjfeng@lut.cn

Received: 25 January 2018 / Accepted: 20 March 2018 / Published: 10 May 2018

Lithium-sulfur batteries have a high theoretical energy density and are low-cost and environmentally friendly. However, the use of low-activity materials and the poor cycle stability of lithium-sulfur batteries severely restrict their application. Here, we prepared a highly porous honeycomb-like carbon (PHC) in two very simple steps, including the mixing of ammonium chloride and sucrose and a straightforward carbonization process. With PHC as the sulfur host, the PHC/S cathode exhibited excellent cycle stability, a high initial discharge capacity of 1200 mAh g⁻¹ at 0.1 C and a retentive capacity of 81% after 200 cycles at 0.2 C. These excellent properties can be attributed to the abundant interconnected mesopores, which prevented the shuttling of polysulfides and provided spacious channels for the transportation of electrons and lithium- ions.

Keywords: Lithium-sulfur battery; cathode; sugar blowing; porous honeycomb-like carbon

1. INTRODUCTION

In recent years, lithium-ion batteries (LIBs) have been widely studied across many fields because of their high energy densities. However, the capacities of current LIBs are limited, and their theoretical values have been nearly reached. As such, it is important to develop new storage devices with high energy densities. Li-S batteries have been considered one of the most promising next-generation batteries because they have a high theoretical capacity (1675 mAh g⁻¹) and are both , low - cost and environmentally friendly materials; consequently, in-depth research on these materials has been performed in the past decade [1–3]. However, the commercial application of Li-S batteries faces several serious problems: (1) the poor conductivity of sulfur and the discharge product Li₂S; (2) the high solubility of polysulfides in organic liquid electrolytes, results in a “shuttle effect” that is driven

by the concentration gradient force and electric field from the anode to the cathode, as well as the sulfide sediment on the lithium anode surface. As a result, a serious attenuation of the capacity of the sulfur cathode can be detected as the battery charges and discharges; (3) the volume expansion between polysulfides and sulfur causes the active substance to detach from the cathode.[4,5].

In recent years, researchers have employed various strategies to combat these problems and improve the performance of Li-S batteries. Porous carbons, metal-organic frameworks, metal-sulfides and their conductive properties have been extensively studied, and these materials have been applied as sulfur hosts in Li-S batteries[6–9]. In particular, high conductivity nitrogen/sulfur co-doped graphene sponges[10], 3D graphene nanosheets@carbon nanotube matrices[11], 3D graphene frameworks[12] and other three-dimensional carbon frame structures[12–14] have been used as sulfur hosts to improve the performance of Li-S batteries. However, graphene, carbon nanotubes, graphene@CNT composites and their associated carbon frame structures are usually sourced from high-cost materials and require complex preparation processes. Compared to those materials, porous carbons are more promising from a practical perspective due to their remarkable physicochemical properties, high surface area, rich porosity and high electronic conductivity[2]; because of these properties, these materials can act as excellent absorbers for polysulfides to improve the performance of Li-S batteries. As a result, it is very important to develop simple, low-cost preparation methods for porous carbon.

Sugar is sourced from a wide range of carbohydrates, and is commonly used in a variety of fields due to its low cost and well-developed preparation processes. Sugar melts to a viscous liquid at 160 °C. Ammonium chloride vigorously decomposes at the same temperature to produce a large amount of ammonia. Inspired by the ancient food art of ‘blown sugar’, Yoshio Bando[15] used sugar and ammonium to develop a sugar-blowing technique to grow 3D self-supported graphene products. Yuehe Lin[16] used a similar method to prepare phosphide/nitrogen-doped carbon nanostructures as catalysts for the enhanced electrochemical oxidation of water and other small molecules. Carbon nanocages[17] and graphitic carbon nitride[18] have also been prepared by the same method and showed excellent electrochemical performance.

Herein, inspired by this previous work, we report a facile sugar-blowing method to prepare a porous honeycomb-like carbon (PHC) as a sulfur host for Li-S batteries. We studied the morphology and electrochemical performance of the PHC/S composite. While the mixture of sugar and NH_4Cl was heated, the decomposition of NH_4Cl released many gases, which blew a rope-like fused material of sugar and generated numerous polymer bubbles. Finally, the porous honeycomb-like carbon (PHC) was synthesized with a carbonization process. As the sulfur host in a Li-S battery, the high porosity and large surface area of PHC can afford relatively strong adsorption of polysulfides, reduce the damage to the cathode materials from volume expansion and provide capacious channels for the transportation of electrons and lithium-ions as the battery is charged and discharged.

2. EXPERIMENTAL

2.1. Preparation of the PHC/S composite

The PHC was prepared by a two-step sugar blowing method. Typically, 2 g sucrose (99%, AR, Shanghai Chemical Reagent Company, SCRC) was mixed well with 1 g NH_4Cl (99%, AR, SCRC),

heated with a heating rate of 4 °C/min and finally annealed at 1000 °C for 3 h under an Ar atmosphere in a tube furnace (130 cm length by 6 cm diameter). After milling, the sample was washed by alternating deionized water and ethanol and dried thoroughly in a dryer at 60 °C. The PHC/S composites were prepared by the traditional melt diffusion method. The prepared PHC and sulfur powder (99.5% AR, SCRC) in a ratio of 1:3, respectively, were ground together for 30 min. Then, the mixture was processed by heating at 155 °C for 12 h in an Ar atmosphere. After annealing, the PHC/S composite was obtained.

2.2. Characterization Methods

The crystal phases of all the samples were characterized by powder X-ray diffraction (XRD, Rigaku Corporation Tokyo, Japan) using a Bruker D8 Advance diffractometer with Cu K α radiation from 10° to 90°. The surface images of the sample were taken by scanning electron microscopy (SEM, JSM-6700F, JEOL, Tokyo, Japan) at 20 kV. The interior morphology was characterized by transmission electron microscopy (TEM, JEM-2100F, JEOL, Tokyo, Japan) at 200 kV. The sulfur content of S/PHC composite was measured by thermogravimetric analysis (TGA, STA449C, NETZSCH, Germany).

2.3. Preparation of cathode and electrochemical measurements

The PHC/S composite, super P carbon black, and polyvinylidene fluoride (PVDF) at a ratio of 70:20:10 by weight were ground in a mortar for 30 min with *n*-methyl-2-pyrrolidinone (NMP) as the solvent. Then, the uniform slurry that formed was coated onto aluminum foil and dried at 55 °C for 12 h in a vacuum oven to obtain the cathode. The electrochemical performance of the PHC/S composite was detected by assembling a CR2025 coin cell with lithium foil of 15.8 mm as the counter electrode. The electrolyte was composed of 1 M L⁻¹ lithium hexafluorophosphate (LiTFSI) 1,3-dioxolane (DOL) and DME (1:1 by volume) with 1 wt% LiNO₃ (Xiaoyuan Energy Technology Inc., Shanghai, China). The Celgard 2400 was the separator on the top of the electrode, and 50 μ L of electrolytes were added in each cell. A Land CT2001A battery test instrument (LANHE Inc., Wuhan, China) was used for the charge-discharge performance tests with a 1.5 V to 2.7 V voltage range (versus Li/Li⁺) at room temperature. The CV measurement was carried out with a CS350 Electrochemical workstation (Corrtest Inc., Wuhan, China) in the range of 1.5-2.7 V at a scanning rate of 0.1 mV s⁻¹.

3. RESULTS AND DISCUSSION

3.1 SEM and TEM characterization of the PHC

Figure 1a shows a schematic diagram of the preparation of PHC. The rationale for this preparation method can be confirmed by the SEM and TEM images. Figure 1b and 1c show the SEM

images of PHC. An abundant honeycomb-like, porous, hollow structure with pore diameters in the micron range is clearly observed.

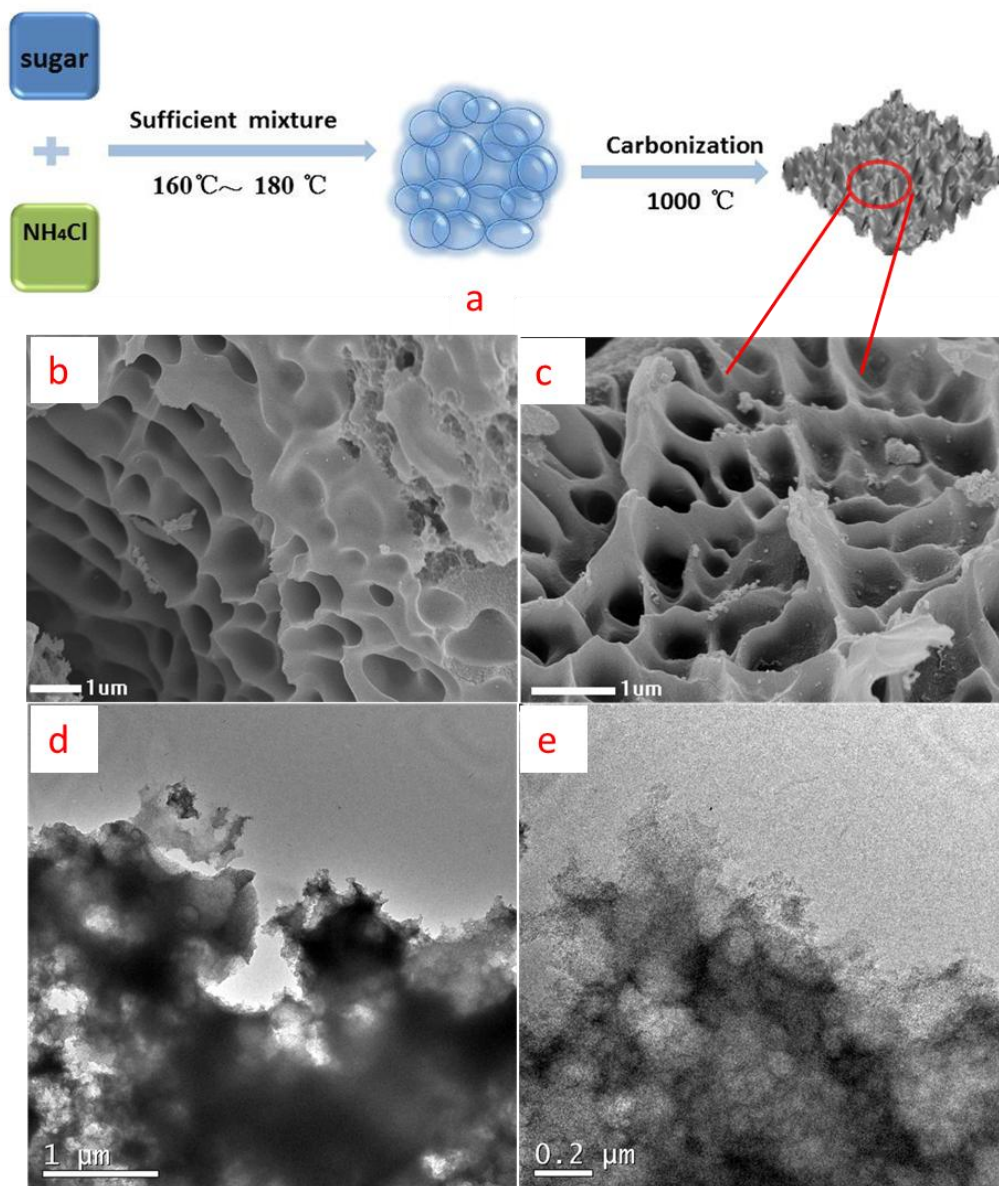


Figure 1. (a) Schematic of the preparation of PHC, (b) (c) SEM images of PHC, (d) (e) TEM images of PHC

This structure originated from the gases that were formed during the decomposition of NH_4Cl while blowing the melted sucrose at $160\text{ }^\circ\text{C}$. This unique morphology contributed to the higher surface area, which allowed more locations for both sulfur loading and the adsorption of polysulfides. Figure 1d and 1e display the TEM images of PHC, which also showed a honeycomb-like porous hollow structure, which is in agreement with the SEM characterization.

3.2 XRD, TGA and elemental analysis of PHC/S

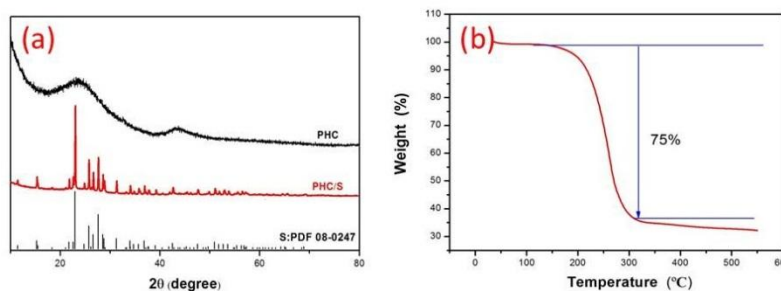


Figure 2. (a) XRD patterns of PHC and the PHC/S composite, (b) TGA curve of the PHC/S composite

The crystallographic phases of PHC and the PHC/S composite were analyzed by XRD (Fig. 2a). The characteristic phases of PHC showed two broad peaks approximately between 24° and 44°, which indicated amorphous PHC characteristics and partially graphitized carbon of the PHC, respectively [14,19]. The diffraction patterns of PHC/S showed the same pattern as pure sublimed sulfur (PDF 08-0247), indicating that elemental sulfur was uniformly distributed throughout the pores and the surface of the PHC. The thermogravimetric analysis (TGA) indicated that the sulfur content of the PHC/S composite is ~75 wt% (Fig. 2b). The relatively high sulfur content is mainly due to the abundant honeycomb-like porous hollow structures of the PHC.

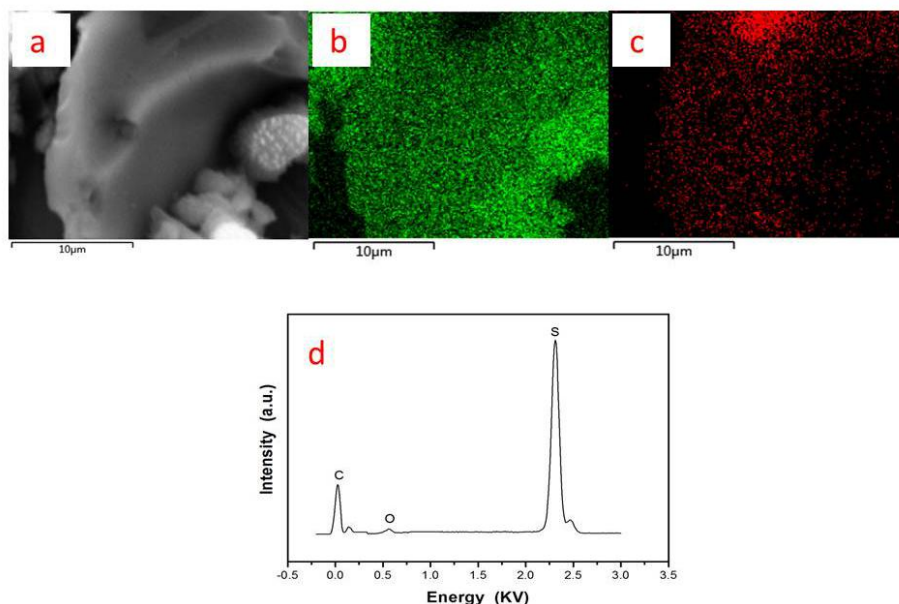


Figure 3. (a) SEM images of PHC/S; (b, c) EDS mappings showing the distribution of C and S; (d) Elemental analysis

After a melt infiltration treatment at 155°C, the PHC/S composite was obtained (Figure 3a). The EDS elemental mapping of PHC/S are shown in Fig. 3b and 3c. A high sulfur content with a uniform distribution can be detected in the scan area. The relatively small amount of PHC provides a

conductive framework for the sulfur electrode and ample channels for the lithium-ions during the charging or discharging process. Furthermore, the elemental analysis by EDS (Fig. 3d) of PHC/S further confirmed the relative contents of internal S and C in the PHC/S.

3.3 The XPS analysis

To explore the chemical activation of PHC/S, X-ray photoelectron spectroscopy (XPS) measurements were acquired. In Fig. 4a, the full XPS spectra of PHC/S shows three peaks at 163.6, 284.69, and 531.6 eV, corresponding to S2p, C1s and O1s, respectively. In the high-resolution XPS spectra of PHC/S, the C1s (Fig. 4b) exhibits two peaks at 284.96 and 285.69 eV, corresponding to sp^2 hybridized carbon and C-S bonds[20]. The S2p (Fig. 4c) spectra of the PHC/S composite can be characterized by four peaks at 163.6, 164.8, 165.9 and 186.6 eV, corresponding to S2p_{3/2}, S2p_{1/2}, S-O, and sulfate. The two prominent peaks correspond to the S2p_{3/2} and S2p_{1/2} from the spin-orbit coupling of the C-S-C covalent bond in the thiophene S. The low-intensity peak at 186.6 eV binding energy was assigned to sulfates such as C-SO_x-C ($2 \leq x \leq 4$) bonds[21–24]. The analysis of the XPS spectra infers that the sulfur and porous carbon are bound by strong chemical bonds after the heat treatment of the mixture of PHC and sulfur. This strong chemical interaction is likely to adsorb polysulfides during charging and discharging, which will further improve the electrochemical performance of the PHC/S electrode.

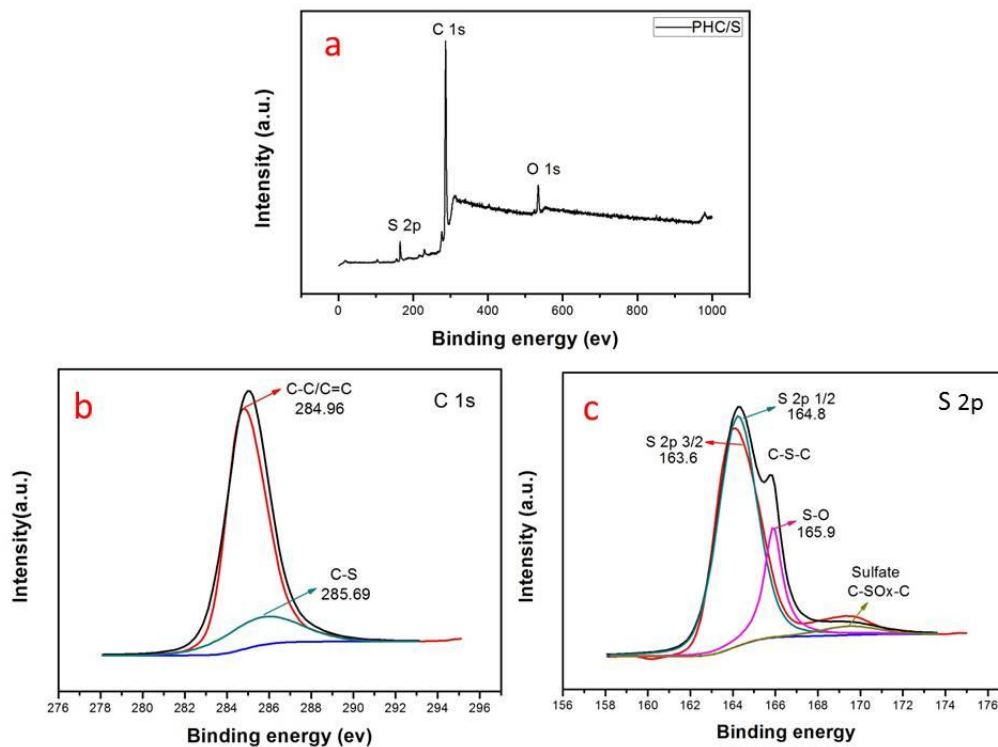


Figure 4. (a) XPS spectrum of PHC/S; High-resolution XPS spectra of (b) C1s, (c) S2p.

3.4 Electrochemical performance

Electrochemical measurements were carried out to evaluate the performance of the PHC/S cathode. Figure 5a shows the charge/discharge capacity of the PHC/S cathode, which delivered discharge capacities of 1200 mAh g^{-1} , 835 mAh g^{-1} , 729 mAh g^{-1} , 572 mAh g^{-1} , 380 mAh g^{-1} and 180 mAh g^{-1} at a rate of 0.1 C, 0.2 C, 0.5 C, 1 C, 2 C and 3 C, respectively. As shown in the charge/discharge profiles, a typical double discharge platform was displayed during the first cycles at increasing charge/discharge rates from 0.5 C to 2 C. An obvious attenuation can be observed from the 0.1 C to 0.2 C cycles, probably because of an activation process during the first few cycles and the formation of a solid electrolyte interface (SEI) on the surface of the lithium anode. The formation of this SEI film partially consumes the lithium ions and causes the irreversible capacity of the first charge-discharge event. The second discharge platform disappeared in the charge-discharge curve at the rate of 3 C, which was mainly because the transfer rate of electrons is much larger than the transfer rate of lithium ions at high current, meaning the solid phase Li_2S_2 can't be formed in time.

Figure 5b displays the cyclic voltammograms (CV) of the PHC/S cathode at a scanning rate of 0.1 mV s^{-1} . Two cathodic peaks are observed, which correspond to the typical two-step reduction of sulfur. The higher potential peak (I) corresponds to the conversion of sulfur rings (S_8) to long-chain polysulfides (Li_2S_n , $4 \leq n \leq 8$). The lower potential peak (II) corresponds to the conversion of long-chain polysulfides to solid phase Li_2S_2 and Li_2S [25]. Theoretically, if all the polysulfides formed Li_2S , the ratio of the areas of II/I would be 3[26]. From Fig. 5 b, the ratio of the areas of II/I is 2.4 (calculated by Origin 8.0), implying that there was a higher transfer efficiency between the soluble long-chain polysulfides to the insoluble $\text{Li}_2\text{S}_2/\text{Li}_2\text{S}$ during the discharge process. The anodic peak (III) corresponds to the conversion of Li_2S to polysulfides, and eventually to S_8 [26].

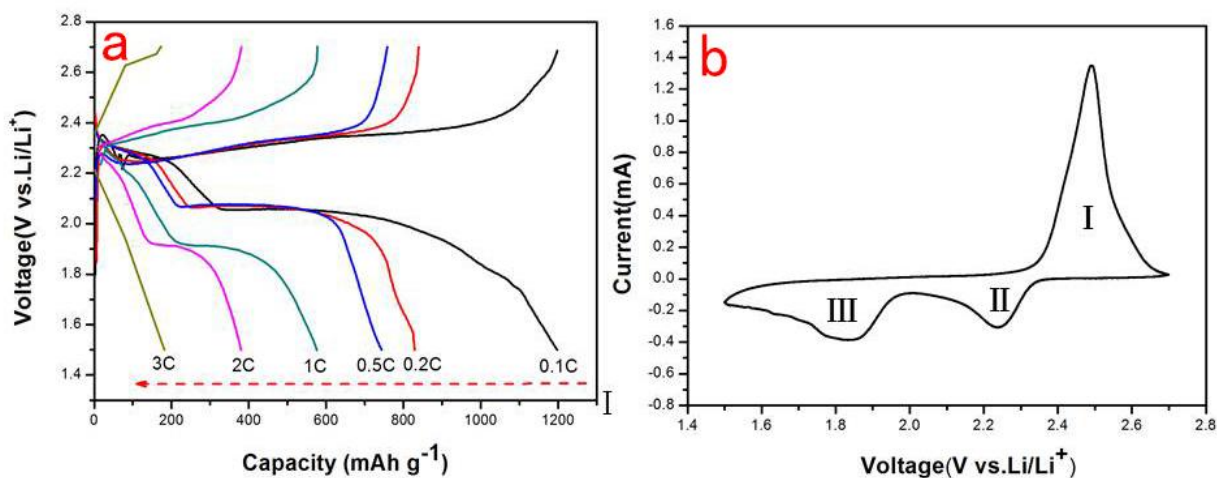
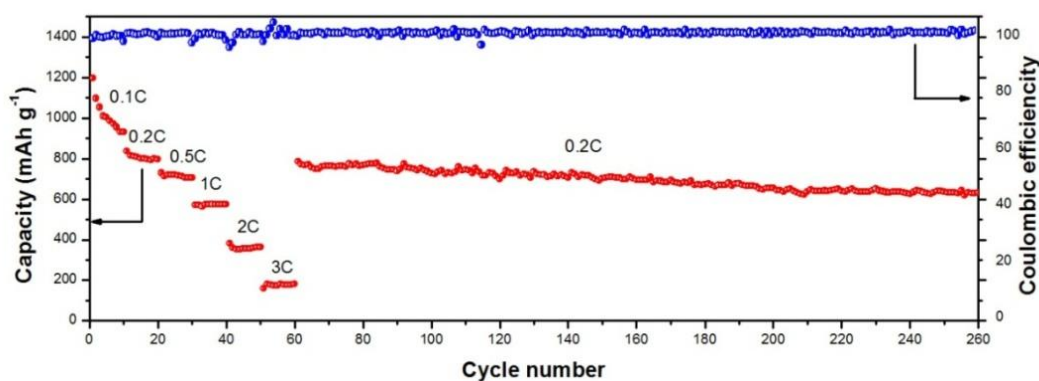


Figure 5. (a) Charge/discharge profiles of the PHC/S cathode at 0.1 C, 0.2 C, 0.5 C, 1 C, 2 C and 3 C charge/discharge rates; (b) CV profile of the PHC/S cathode at 0.1 mV S^{-1}

Table 1. Comparison of this work to other reported porous carbon cathodes for Li-S batteries

Raw materials	Morphology	Preparation process	Capacity retention (200 cycles)	Ref
Graphene	Micron frameworks	complex	90% (1C)	[12]
Popcorn	Macrocellular	complex	80% (0.2C)	[14]
Egg shell	Mesoporous	simple	68% (2C)	[15]
Poplar catkin	Mesoporous	simple	70% (0.1C)	[24]
CNT and Na ₃ C ₆ H ₅ O ₇	Interconnected porous carbon	complex	59% (2C)	[17]
Sugar and NH ₄ Cl	Honeycomb-like carbon	very simple	81% (0.2C)	This work

Figure 6 presents the rate stability and cycle stability of the PHC/S composite. The gradual reduction in discharge capacity of the PHS/S cathode can be clearly observed as the current density rate increases from 0.1 to 3 C. A reversible capacity of 180 mAh g⁻¹ and good cycle stability were maintained even at the high current densities of 3 C. When the charge/discharge current returned to 0.2 C, the PHC/S composite exhibited a reversible capacity of 781 mAh g⁻¹, which remained at 634 mAh g⁻¹ after 200 cycles, corresponding to a capacity retention of 81%. The PHC/S composite cathode presents high coulombic efficiencies ($\geq 98\%$) at all tested current rates, indicating that the polysulfide shuttle effect has been sufficiently suppressed by the porous honeycomb-like architecture of the carbon used as the sulfur host. In addition, the extensive interconnected mesopore-structures not only prevent the dissolution of polysulfides but also may improve the immersion and permeation of the electrolyte into the active materials[27]. As a result, PHC/S composite material exhibits a high rate performance and excellent cycle stability as the cathode in a lithium-sulfur battery. In comparison to previously reported porous carbon cathodes (Table 1), our work provided an easy method for preparing cathodic materials for lithium-sulfur batteries. The inexpensive starting materials, easy preparation process, and excellent electrochemical performances of PHC/S cathodes make these materials good candidates for the industrial application of lithium-sulfur batteries.

**Figure 6.** Rate stability and cycle stability of the PHC/S composite.

4. CONCLUSION

In conclusion, the preparation of a unique porous honeycomb-like carbon/sulfur (PHC/S) cathode and its application in lithium-sulfur batteries were reported in this paper. The abundant interconnected mesopores prevent the dissolution of polysulfides and provide spacious channels for the transportation of electrons and Li^+ . The PHC/S composite exhibits better electrochemical performance than other porous carbon cathodes for Li-S batteries, showed a high initial discharge capacity of 1200 mAh g^{-1} at 0.1 C, displayed a high rate performance of 180 mAh g^{-1} at 3 C and had excellent cycle stability with a capacity retention of 81% after 200 cycles at 0.2 C. In comparison to many previous reports of porous carbons for lithium-sulfur batteries, our study provides a simple and feasible synthetic strategy using low-cost materials to achieve stable lithium-sulfur batteries with long lifetimes.

ACKNOWLEDGEMENTS

This work was financially supported by the National Natural Science Foundation of China (Grant No.11264023) and the Natural Science Foundation of the Gansu Province, China (Grant No. 1210ZTC035).

References

1. D. Eroglu, K. R. Zavadil and K. G. Gallagher, *J. Electrochem. Soc.*, 162 (2015) A982.
2. W. Ai, W. Zhou, Z. Du, Y. Chen, Z. Sun, C. Wu, C. Zou, C. Li, W. Huang and T. Yu, *Energy Storage Mater.*, 6 (2017) 112.
3. J. Lochala, D. Liu, B. Wu, C. Robinson and J. Xiao, *ACS Appl. Mater. Interfaces*, 9 (2017) 24407.
4. G. Li, J. Sun, W. Hou, S. Jiang, Y. Huang and J. Geng, *Nat. Commun.* 7 (2016) 10601.
5. A. Manthiram, Y. Fu and Y.-S. Su, *Acc. Chem. Res.*, 46 (2013) 1125.
6. C. Ye, L. Zhang, C. Guo, D. Li, A. Vasileff, H. Wang and S.-Z. Qiao, *Adv. Funct. Mater.*, 27 (2017) 1702524.
7. Z. Li, C. Li, X. Ge, J. Ma, Z. Zhang, Q. Li, C. Wang and L. Yin, *Nano Energy*, 23 (2016) 15.
8. Z. Yuan, H.-J. Peng, T.-Z. Hou, J.-Q. Huang, C.-M. Chen, D.-W. Wang, X.-B. Cheng, F. Wei and Q. Zhang, *Nano Lett.*, 16(2016) 519.
9. J. Park, B.-C. Yu, J. S. Park, J. W. Choi, C. Kim, Y.-E. Sung and J. B. Goodenough, *Adv. Energy Mater.*, 7 (2017) 1602567.
10. G. Zhou, E. Paek, G. S. Hwang and A. Manthiram, *Nat. Commun.*, 6 (2015) 7760.
11. Z. Zhang, L.-L. Kong, S. Liu, G.-R. Li and X.-P. Gao, *Adv. Energy Mater.*, 7 (2017) 1602543.
12. R. Fang, S. Zhao, P. Hou, M. Cheng, S. Wang, H.-M. Cheng, C. Liu and F. Li, *Adv. Mater.*, 28 (2016) 3374.
13. Y. Zhong, X. Xia, S. Deng, J. Zhan, R. Fang, Y. Xia, X. Wang, Q. Zhang and J. Tu, *Adv. Energy Mater.*, (2017), 1701110.
14. X. Yuan, L. Wu, X. He, K. Zeinu, L. Huang, X. Zhu, H. Hou, B. Liu, J. Hu and J. Yang, *Chem. Eng. J.*, 320 (2017) 178.
15. X. Wang, Y. Zhang, C. Zhi, X. Wang, D. Tang, Y. Xu, Q. Weng, X. Jiang, M. Mitome, D. Golberg and Y. Bando, *Nat. Commun.* 4 (2013) 2905.
16. C. Zhu, S. Fu, B. Z. Xu, J. Song, Q. Shi, M. H. Engelhard, X. Li, S. P. Beckman, J. Sun, D. Du and Y. Lin, *Small*, 13 (2017) 1700796.
17. X. X. Wang, B. Zou, X. X. Du and J. N. Wang, *J. Mater. Chem. A*, 3 (2015) 12427.
18. X. Lu, K. Xu, P. Chen, K. Jia, S. Liu and C. Wu, *J Mater Chem A*, 2 (2014) 18924.

19. B. Zhang, X. Qin, G. R. Li and X. P. Gao, *Energy Environ. Sci*, 3 (2010) 1531.
20. S. Yuan, Z. Guo, L. Wang, S. Hu, Y. Wang and Y. Xia, *Adv. Sc.*, 2 (2015) 1500071.
21. X. Yu and H. S. Park, *Carbon*, 77 (2014) 59–65.
22. Y.-X. Wang, L. Huang, L.-C. Sun, S.-Y. Xie, G.-L. Xu, S.-R. Chen, Y.-F. Xu, J.-T. Li, S.-L. Chou, S.-X. Dou and S.-G. Sun, *J. Mater. Chem*, 22 (2012), 4744.
23. J. Yang, S. Wang, Z. Ma, Z. Du, C. Li, J. Song, G. Wang and G. Shao, *Electrochim. Acta*, 159 (2015) 8.
24. Y. Zhao, J. Ren, T. Tan, M.-R. Babaa, Z. Bakenov, N. Liu and Y. Zhang, *Nanomaterials*, 7 (2017) 260.
25. D.-W. Wang, Q. Zeng, G. Zhou, L. Yin, F. Li, H.-M. Cheng, I. R. Gentle and G. Q. M. Lu, *J. Mater. Chem. A*, 1 (2013) 9382.
26. R. Fang, S. Zhao, S. Pei, X. Qian, P.-X. Hou, H.-M. Cheng, C. Liu and F. Li, *ACS Nano*, 10 (2016) 8676–8682.
27. J. Wu, J. Hu, K. Song, J. Xu and H. Gao, *J. Alloys Compd*, 704 (2017) 1

© 2018 The Authors. Published by ESG (www.electrochemsci.org). This article is an open access article distributed under the terms and conditions of the Creative Commons Attribution license (<http://creativecommons.org/licenses/by/4.0/>).